Self-generating magnetometer with laser pumping employment in "end resonance" wall coated vapor cell atomic clocks

A A Baranov, S V Ermak, R V Smolin and V V Semenov

Department of Quantum Electronics, Peter the Great St. Petersburg Polytechnic University, St. Petersburg, Russia

Vladimir_semenov@mail.ru

Abstract. This paper presents the results of two double resonance signals correlation investigation. These signals were observed synchronously in optically oriented Rb^{87} vapors with laser pumping in a dual scheme: low frequency M_x-magnetometer and microwave frequency discriminator. Analytical studies of the scalar and vector light shift components contribution to the frequency instability of the end resonance microwave transitions are presented. An experimental demonstration of the light shift components mutual compensation in optically pumped Rb^{87} atoms was provided. The results were processed in terms of Allan variance, which demonstrated an effect of decreasing frequency variation at averaging times more than 100 s for a joint scheme of the end resonance microwave transition and self-generating (M_x) magnetometer.

1. Introduction

The light shift of the energy sublevels caused by incident electromagnetic optical field is one of the major sources of instability of precision quantum devices such as alkali vapor cell frequency standards and quantum magnetometers with optical pumping.

The light shift theory developed in fundamental work [1] shows that frequency shift observed in experiments with alkali atoms vapors contains three components:

- The scalar shift, which is identical for all magnetic sublevels of a hyperfine structure F or F*.
- The vector light shift, caused by an effective magnetic field due to circular polarized light (an inverse Faraday Effect).
- Tensor light shift caused by ground state atoms alignment. It depends on a magnetic quantum number m_F.

Their weights are determined by pumping source spectrum and ground-state magneto-dipole transition type.

Scalar and tensor components are observed on a microwave transition between sublevels with different quantum number F. Vector and tensor components appear in quantum magnetometers working on Zeeman transitions between nearest sublevels in magnetic structure of a ground state in presence of a circular polarized light. The value of the tensor component as opposed to the scalar component depends on an angle θ between the C-field and the pumping light directions. When the tensor component is small enough to neglect, depending on the sign of the circular polarization of the pumping light (the direction of the effective magnetic field) the scalar and vector components of the light shift will either be folded or subtracted, which leads to the possibility of their mutual

compensation, which in turn allows to reduce the influence of the pumping source on a quantum device frequency stability. It should be emphasized that such compensation is possible only for magnetically dependent transitions, whereas for microwave 0-0 transition used in atomic clocks vector component of the light shift is absent. In this paper we analyze the contribution of the vector and scalar components to the frequency shift of microwave magnetic dependent transitions, and provide an experimental demonstration of the compensation of these components with respect to the optical orientation of the Rb^{87} atoms with laser source tuned to the D_2 line of the doublet (figure 1a). D_2 line was chosen because of the opportunity to neglect the tensor component of the light shift, which in the case of the D_1-line pumping, plays an essential role [2].

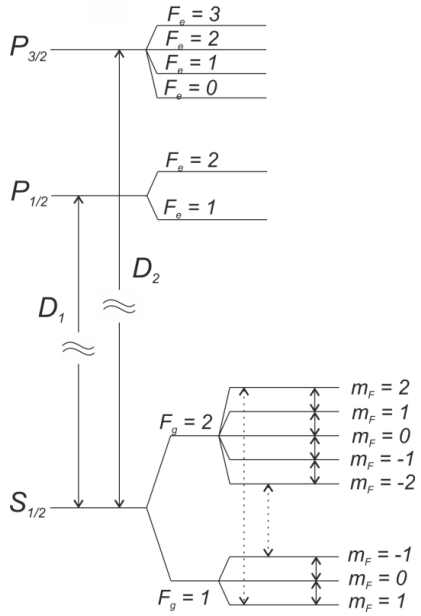

Figure 1a. Rb^{87} atom simplified energy levels system.

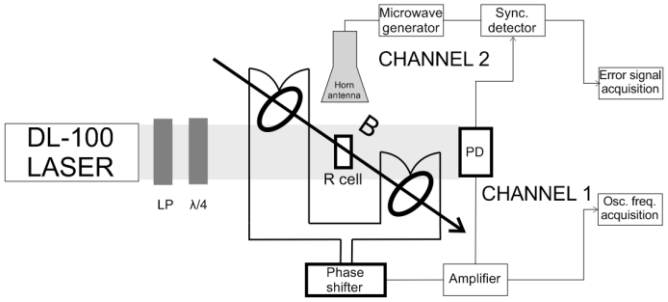

Figure 1b. Simplified experimental setup of the magnetometer joint scheme.

2. Theory

Analytical expressions for the components of the light shift for 0-0 microwave transition practiced in atomic frequency standards were obtained in [1]. In this paper, the analytical aspect was focused on the so-called "end resonance" transitions between hyperfine sublevels with extreme values of the magnetic quantum number [3]. Using the formalism [1], we can obtain the following expression for the tensor components of the light shift:

$$S_T = -\frac{2\pi}{hc}\left(1-3\cos^2\theta\right)\sum_{F_g}\sqrt{5}\left\{\frac{3m_F^2 - F_g\left(F_g+1\right)}{\left[\left(2F_g+3\right)\left(F_g+1\right)\left(2F_g+1\right)F_g\left(2F_g-1\right)\right]^{1/2}}\right\}\mathrm{Re}\,A^2\left(F_g,F_g\right)\left(-1\right)^{I+1/2-F_g}, \quad (1)$$

where

$$A^2\left(F_g,F_g\right)=\frac{3\lambda^2 r_0 f_{ge}}{4\pi^2}\left[\frac{Mc^2}{2RT}\right]\left(2F_g+1\right)\sum_{F_g}\left(2F_e+1\right)W\left(11F_g,F_g;2F_e\right)W^2\left(J_eF_e\frac{1}{2}F_g;I1\right)Z\left(F_e,F_g\right)(-1)^{F_e-F_g-1} \quad (2)$$

$$Z\left(F_eF_g\right)\equiv Z\left[x\left(F_eF_g\right)+iy\right] \quad (3)$$

– form-factor of the Doppler broadened resonance line expressed in terms of plasma-dispersion function of the arguments x and y

$$x\left(F_eF_g\right)=\frac{1}{\nu}\left(\frac{Mc^2}{2RT}\right)^{1/2}\left\{\left[\nu-\nu_{cg}\right]-\left[\nu\left(F_eF_g\right)-\nu_{cg}\right]\right\} \quad (4)$$

$$y=\left(\frac{Mc^2}{2RT}\right)^{1/2}\left(\frac{1/2\tau+\gamma_c}{2\pi\nu}\right) \quad (5)$$

$W(11F_g,F_g;2F_e)$ - Racah coefficient, M – atomic mass, c– light velocity, R – gas constant, T – temperature, τ - excited state life time, γ_c – is determined by alkali atoms and buffer gas atoms colliding frequency, F_e and F_g – mechanical moments in the ground and excited states, f_{eg} – oscillator force, r_0 – classical electron radius, λ and ν pumping source wavelength and frequency, ν_{cg} – weighted frequency of electro-dipole transition.

S_T is a normalized to the pumping light intensity ground state frequency shift, which corresponds to the tensor component of the Light shift operator [1]. Equation (1) was derived from dipole matrix elements, which characterize the interaction between non-resonant optical field and Rb^{87} atoms. These elements were written as a product of Clebsch-Gordan coefficients and reduced matrix elements (Wigner-Eckart theorem) and further simplified with Racah-coefficients implementation. Final expression of the spectral response function (1) depends on an angle θ between magnetic field direction and light propagation, magnetic-dipole transition choice, absorption line profile and transition probability. Physically it is related to a transition resonance frequency shift caused by different transition probabilities for atoms with different magnetic quantum number projection.

Figure 2a and 2b demonstrate examples of Rb^{87} atoms spectral responses calculation under the influence of circularly polarized monochromatic radiation of the laser source tuned to the D_1 and D_2 line. The graphs show that the sign of the circular polarization of the pump light can significantly reduce the overall spectral response of an alkali atom due to the compensation of the scalar component of the light shift by the vector component.

3. Experiment

The light shift compensation effect was experimentally checked under the condition of the laser pumping of Rb^{87} by the long-wavelength component of the D_2 line in a dual scheme: self-oscillating M_x-magnetometer and end resonance microwave frequency standard. The experiments were performed on a laboratory setup of a quantum discriminator, which contains a well-known set of components [4] and a 1 cm^3 Rb^{87} cell with anti-relaxation coated walls. An experimental setup shown on Figure 1b combines two types of quantum magnetometers with a single optical trunk: the first is an M_x-magnetometer (self-oscillating magnetometer) and the second is a microwave “end resonance” magnetometer. The working frequency of the spin oscillator is determined by the weighted mean low frequency (Larmor frequency) of the magneto-dipole transitions between Zeeman sublevels in the Rb^{87} ground state structure. This frequency can be translated to magnetic field units using a well-known gyromagnetic equation $w=\gamma H$. Microwave frequency of the second magnetometer depends on the pumping light polarization choice and equals approx. 6.834 GHz. Error signal in this channel is used to determine the microwave generator and atomic transition frequency difference. As magnetic dependent “end resonance” transition was chosen, the error signal value is a measure of magnetic field variations. Resonance cell was placed in the center of the coils producing a working magnetic field (100 nT). To weaken the external magnetic interference and magnetic field inhomogeneity the whole system was placed in a two-layer magnetic shield with a shield factor 100. Microwave field, which induces transitions in the hyperfine structure of rubidium atoms was produced by frequency

multiplication of the reference crystal oscillator followed by amplification of the signal in the microwave amplifier. A horn antenna was utilized to create a required microwave field distribution in the resonance cell.

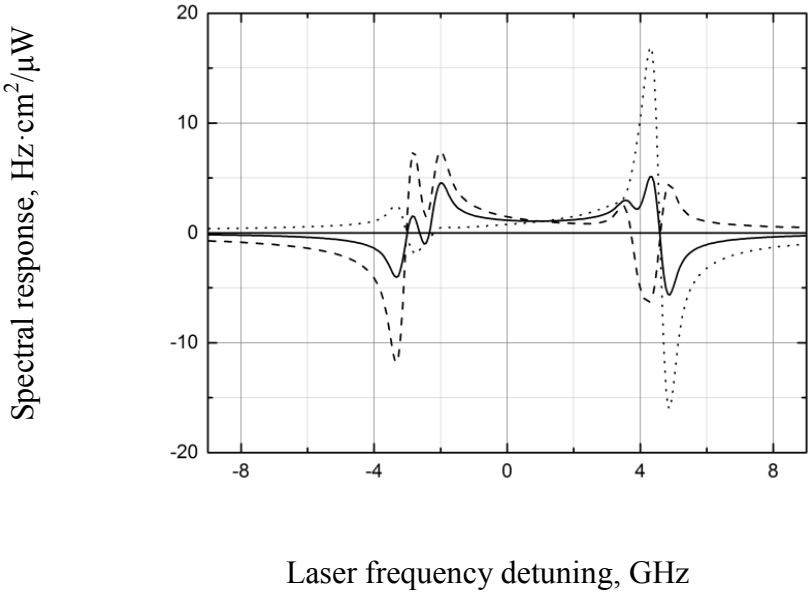

Figure 2a. Rb^{87} D_1-line spectral response: solid line – scalar component; dashed line – σ^- polarization (light shift components residual); dotted line - – σ^+polarization (light shift components superposition).

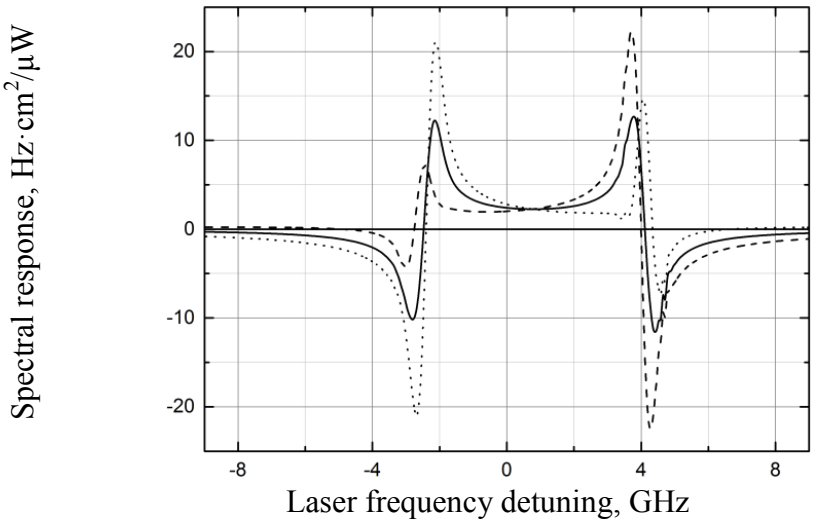

Figure 2b. Rb^{87} D_2-line spectral response: solid line – scalar component; dashed line – σ^- polarization (light shift components residual); dotted line - – σ^+polarization (light shift components superposition).

Along with the microwave signal a low frequency spin generator signal at Larmor precession frequency was induced at photodetector. The experiment showed significant interference of the LF and microwave signals, determined as changes in the dynamics of their intensity and spectral composition.

The difference between the synchronously recorded signals in a dual scheme normalized to uniform measurement units (nT) was processed to determine the Allan variance as a function of averaging time (an example of such a record is presented in figure 3).

The correlation coefficient between the detected signals in the dual scheme depends on the pumping rate and RF fields intensity in the vapor cell area. Depending on the intensity of the applied fields and the power of the spin generator self-oscillation correlation coefficient varied in a range of 0.3 - 0.98.

The optimal (the best long-term stability of the dual scheme) parameters of the fields were determined experimentally. In particular, for the wall coated cells optimal parameters in terms of the line broadening with respect to the microwave resonance dark line width (about 200 Hz) are: 20% - pumping light, 20% - of the microwave field, and 10% - spin RF generator. The last recommendation corresponds to half maximum of self-oscillations level in a spin system saturation mode.

Interference of microwave and LF signals appeared in a spin generator frequency shift due to microwave transition frequency variation which physics is not related to variations of the magnetic field. Such a shift is caused by coherence circulation between the sublevels of the hyperfine structure of alkali atoms "dressed" by LF field of the spin generator and depends on the sign of the circular polarization of the pumping light, the intensity of the applied field and magnetic dipole transition in the microwave absorption spectrum.

4. Conclusion

It was found that the absolute value of this shift for end resonance transition in the dual scheme is more than an order of magnitude smaller than in the analog tuned to 0-0 transition. In this case, for different pumping light polarization ($\sigma+$ and σ^-) frequency shift of the spin generator was observed with the opposite sign while increasing microwave field detuning from the resonance value.

The workability of the dual scheme was realized only when the laser is tuned to the long-wave component of the electric dipole transition, when the optical field interacts with the maximum number of atoms on the sublevels of the hyperfine structure. Tuning to the short-wavelength laser component of the D_2 line did not give a positive effect due to the breach of the self-excitation condition because of the low concentration of atoms caused by the effect of optical pumping.

Allan deviation plots show a relation between the Light shift of the resonance frequency, which depends on the circular polarization sign, and flicker floor value. SNR was controlled during experiment and its values were equal for left and right circular polarization which means that frequency drift was caused by AC Stark shift, otherwise, for example, in a case of residual magnetic fluctuations presence, flicker floor value should remain constant with polarization change.

As a consequence of scalar and vector components mutual compensation in a dual scheme, Allan variance decreases for hundreds of seconds averaging times in comparison with traditional 0-0 transition atomic clock (Figure 4). In this case, the flicker floor of Allan variance is realized in presence of $\sigma+$ pumping light at much higher averaging times than that observed in a conventional scheme. From the analysis of the effect of flicker processes on technical line width of the spin generator made in [5] follows that for large averaging times t technical line width (and therefore Allan variance) increases according to the law $(t^{n-1})^{1/2}$. Implementing this formula for the dual scheme case an estimated value of the coefficient n is: 2.15 for curve 1, 2.5 for curve 2 and 2.75 for curve 3.

The results allow to conclude that a greater long-term stability can be achieved in a dual scheme compared to traditional 0-0 transition scheme. The effect of the light shift components compensation by changing the sign of laser polarization provides an ability for a more detailed analysis of the pumping source role in the technical noise of a quantum device. In turn that expands the range of optimum designs of device's construction.

Dual scheme operating on a D_1 line can be found interesting to analyse because of sufficient weight of the tensor component of the light shift, which depends on the orientation of the magnetic field with respect to the optical axis [6]. A decrease in the orientation error of atomic devices is expected due to

high degree of correlation of the light shift at microwave and Zeeman transitions, implemented in the dual scheme.

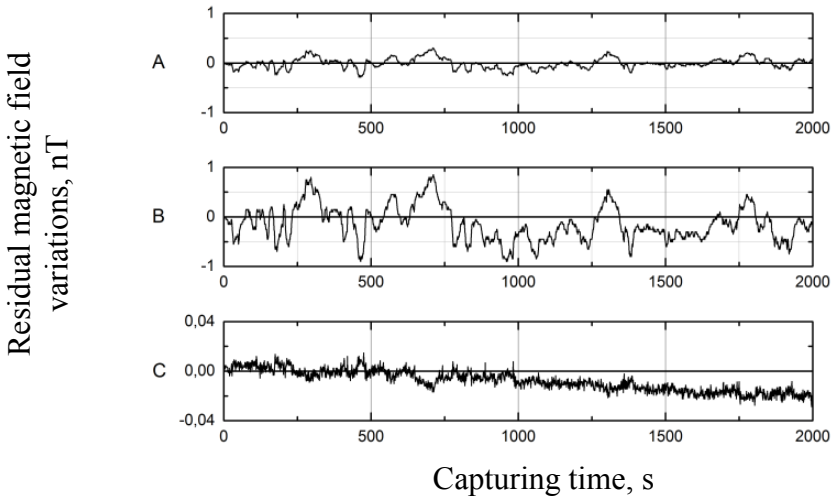

Figure 3. Dual scheme signals capturing: A – low frequency; B – microwave transition; C – residual noise of a dual scheme.

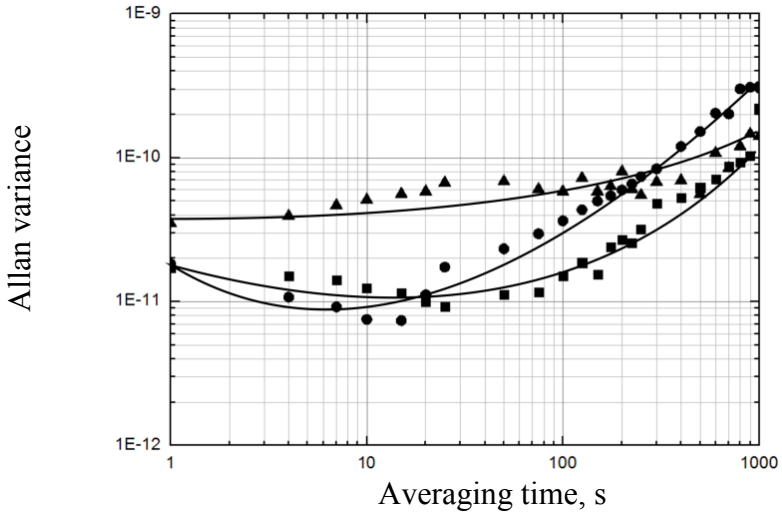

Figure 4. Allan variance for different pumping schemes: rounds (1) – 0-0 transition; triangles(3) – dual scheme (σ+ , optimal light); squares (2) – dual scheme (σ+ , non-optimal light, high quality factor)

References

[1] Happer W, Mathur B S 1967 *Phys. Rev*. **1**, v163.
[2] Semenov V V 1999 *Izv. Vuzov* Physics, **2**.
[3] Jau Y-Y, Post A B, Kuzma N N, Braun A M, et al. 2004 *Phys. Rev. Letters* **11**, 92.
[4] Rihle F 2004 *Frequency Standards: Basics and applications* (Weinheim: WILEY-VCH Verlag GmbH & Co. KGaA).
[5] Semenov V V, Zimnitsii P V, Smolin R V and Ermak S V 2014 *Technical Physics Letters* **3** 40 271-273.
[6] Baranov A A, Ermak S V and Semenov V V 2010 *Nauchno-technicheskie vedomosti SPbSTU* **3** 104.